Direct measurement of singlet oxygen produced by four chlorin-ringed chlorophyll species in acetone solution

Chemical Physics Letter

Direct measurement of singlet oxygen produced by four chlorin-ringed chlorophyll species in acetone solution

Shigetoshi Okazaki[1*], Tatsuya Tomo[2,3], and Mamoru Mimuro[2]

[1]Photon Medical Research Center, Hamamatsu University School of Medicine, Hamamatsu 431-3192, Shizuoka, Japan; [2]Graduate School of Human and Environmental Studies, Kyoto University, Kyoto 606-8501, Japan; [3]Faculty of Science, Tokyo University of Sciences, Kagurazaka, Shinjuku-ku, Tokyo 162-8601, Japan.

*Corresponding author:

Photon Medical Research Center, Hamamatsu University School of Medicine, Hamamatsu 431-3192, Shizuoka, Japan.

Tel: +81-53-435-2235

Fax: +81-53-435-2235

E-mail address: okazaki@hama-med.ac.jp

Abbreviations: Chl, chlorophyll; DV, di-vinyl; MV mono-vinyl; PS, photosystem.

Abstract

We developed an optical system to detect singlet oxygen produced by chlorin-ringed chlorophyll (Chl) species, i.e., Chl *a*, Chl *b*, Chl *d*, and di-vinyl-Chl *a*, with a high sensitivity and examined the relationship between molecular structures and reaction rates. Chl *a* in acetone was the lowest producer of singlet oxygen and the most effective quencher; in contrast, Chl *b* exhibited the opposite properties. These results showed that replacement of side chain(s) from a methyl group to a formyl group on the R7 position on a chlorin ring induced a higher production and lower quenching of singlet oxygen in Chl molecules.

Keywords: Singlet oxygen, Luminescence, Cyanobacteria, Di-vinyl Chlorophyll *a*, Chlorophyll, Photosynthesis

Introduction

Light is an energy source that drives photosynthesis; however, it is also a source of light-induced damages to photosynthetic systems. Photosynthetic organisms, especially oxygenic photosynthetic organisms, develop rescue reactions to protect them from these damages [1]. Photoinhibition is one of the damage reactions that occur in the photosynthetic electron-transfer system [2]; in particular, the acceptor-side inhibition of photosystem (PS) II is a main cause of photodamage [3]. This inhibition is referred to as a sum of several reactions; however, the overall reaction process has not been clarified. This process is initiated by over-reduction of PS II, which induces the charge recombination between the primary electron donor (P680 or accessory chlorophyll (Chl) *a*) and the primary electron acceptor (pheophytin *a*, i.e. demetalated Chl *a*) (scheme); this recombination yields the triplet state of Chl *a* and leads to the production of singlet oxygen via a spin-exchange reaction between the triplet state of Chl *a* and molecular oxygen. This singlet oxygen is harmful to cell components and induces the breakdown of the D1 protein, which is a major functional component of PS II, to form degradation products with a molecular mass of 16 and 8 kDa [4, 5].

Singlet oxygen is one of active oxygen species as similar to hydroxyl radical, super oxide anion radical, and hydrogen peroxide. Singlet oxygen is produced via a photophysical process, whereas the other three active oxygen species are produced via photochemical reactions. Singlet oxygen is detected using luminescence with an emission maximum at 1275 nm (7843 cm^{-1}). As its yield is not high, i.e., less than 10^{-5} in acetone [6], its detection method has been improved to higher sensitivity in the infrared region.

Cyanobacteria are oxygenic photosynthetic prokaryotes that contain Chl *a* as a common pigment (Scheme). Cyanobacteria that contain a novel pigment are produced by introduction of a gene for Chl biosynthesis [7, 8]. The mutant species of *Synechocystis* sp. PCC 6803 (hereafter referred to as *Synechocystis*) accumulates di-vinyl (DV)-Chl *a* instead of

mono-vinyl (MV)-Chl *a* [8, 9] by suppression of the specific enzyme responsible for chlorophyll synthesis, i.e., protochlorophyllide reductase. This transgenic species is sensitive to high light conditions. In addition, cellular DV-Chl *a* and isolated photochemical complexes were bleached within one day under the high light condition [8, 10]. Furthermore, acceptor-side inhibition was observed in the form of degradation products of the D1 protein [9]. It is reasonable to assume that PS II produces a higher amount of singlet oxygen in the presence of DV-Chl *a* compared with MV-Chl *a*. Therefore, we tried to measure the singlet oxygen directly in Chl solutions using luminescence in the infrared region, as a first step in the analysis of the physiological responses to this oxygen species.

There are several reports on the direct measurement of singlet oxygen produced by Chl *a* or Chl *b* in solution [11-14]. In our study, as it was necessary to detect a signal from singlet oxygen in the DV-Chl *a* solution, we developed a detection system with a sensitivity that was adequate for the estimation of the yield of singlet oxygen. In addition to the three Chl species mentioned above, we adopted Chl *d* as a target species to clarify the effect of side-chain replacement in chlorin-ring Chl species on singlet oxygen production. We also examined the correlation of singlet oxygen yield with the molecular structures of the Chl species. This report represents the first description of the properties of production and quenching of singlet oxygen in novel Chl species, i.e., DV-Chl *a* and Chl *d*. We detected species-dependent changes in yield and quenching rates.

Materials and Methods

Culture of algal species

Synechocystis sp. PCC 6803 was cultured under the photoautotrophic condition in BG11 medium at 25°C. The light intensity for growth was adjusted to 25 μmole photon m^{-2} s^{-1} [9]. Air was continuously supplied through a filter (Millex, Millipore, MA, USA). Mutant *Synechocystis* cells containing DV-Chl *a* [8] were cultured in the same medium using the

same illumination conditions as those used to culture wild-type cells. *Acaryochloris marina* MBIC 11017 was cultured in IMK medium under continuous illumination from an incandescent light source (15 μmol photons m^{-2} s^{-1}) at 25°C [15] with continuous supply of air.

Isolation of Chls

Chl *a*, DV-Chl *a*, and Chl *d* were extracted from the thylakoid membranes of *Synechocystis*, a mutant of *Synechocystis*, and *A. marina*, respectively, and Chl *b* was extracted from the thylakoid membranes of spinach. Pigments were extracted using acetone, which was followed by replacement of the solvent with chloroform and purification using high performance liquid chromatography (HPLC; GULLIVER series, JASCO, Tokyo, Japan). Samples were injected into a Senshupak Silica-5301N column (300 mm × 30 mm; Senshu Science, Tokyo, Japan) after filtration (0.2 μm) and were then fractionated. The mobile phase, which was hexane/2-propanol (100:2), was eluted with a flow rate of 5.0 ml min^{-1}. Pigments were detected using a photodiode-array detector (MD- 915, JASCO, Tokyo, Japan). Samples were stored in fused glass vessels and kept in the dark at −80°C until use.

Measurements of singlet oxygen

Emission from singlet oxygen was measured using an apparatus developed and improved for high-sensitivity detection, based on a commercially available apparatus (NIR-PII system, Hamamatsu Photonics K.K., Hamamatsu, Japan, Fig. 1A). The oxygen concentration in acetone solutions was not controlled; however, it was equilibrated with air. The excitation pulse was obtained using a dye laser excited by a Nd:YAG laser (Tempest, New wave research inc., CA, USA). Pulse width and intensity were approximately 10 ns and 300 μJ/pulse, respectively, and the repetition rate was 30 Hz. Emission of singlet oxygen was monitored using an infrared-gated image intensifier (NIR-PII, Hamamatsu Photonics K.K., Hamamatsu, Japan) after passage through a polychromator (250is, Chromex, NM, USA).

Measurements started 5 μs after application of the excitation pulse, and the exposure time was 500 μs. Signals were accumulated by repeated detection (> 300 times) and averaged. Calibration of wavelength was performed using a spectral calibration lamp (Krypton type, Oriel Instruments, CT, USA).

Decay curves of singlet oxygen were monitored using the apparatus shown in Fig. 1B. The light source was an optical parametric oscillator (OPO) (MOPO-HF, Spectra-Physics, CA, USA) combined with a Nd:YAG laser (PRO-250-10, Spectra-Physics, CA, USA). The excitation wavelengths were 662 nm (Chl *a* and DV-Chl *a*), 646 nm (Chl *b*), and 687 nm (Chl *d*). Pulse width and intensity were approximately 8 ns and 300 μJ/pulse, respectively, and the repetition rate was 10 Hz. Emission was detected using a photomultiplier (R5509-42, Hamamatsu Photonics K.K., Hamamatsu, Japan) combined with a monochromator (HR-320, Jobin Yvon, France). Data were stored in a multichannel scaler (SR430, Stanford Research Systems, CA, USA). Decay curves were simulated with two components, i.e., rise and decay component. Rate constants and pre-exponential factors were calculated numerically using the Igor Pro software (Wave Metrics, OR, USA). All measurements were performed at 22°C. Absorption spectra was measured before and after decay measurements to monitor the photobleaching of Chl samples.

Results

Luminescence from singlet oxygen in solution

We detected the luminescence from singlet oxygen at 1275 nm in Chl *a* in acetone (Fig. 2A) under reduced light intensity provided by excitation pulse (300 μJ/pulse), to avoid a saturation effect of absorbed quanta. The signal-to-noise (S/N) ratio of the observed spectra was very high, which underscored the reliability of our measurements. Emission intensities depended on the concentration of samples and there was overlap among the observed spectra (data not shown). The emission spectra of the four Chl samples were superimposable (Fig.

2B), which suggests that the same molecular species was produced. The luminescence intensity depended on the concentration of samples, and we estimated the yield of singlet oxygen production by dividing luminescence intensity by absorbed quanta (Table 1). The relative yields of Chl *b*, Chl *d*, and DV-Chl *a* were 2.24, 1.20, and 1.22, respectively, by normalization to the yield of Chl *a* (1.00). The yields of Chl *d* and DV-Chl *a* were comparable and were intermediary to those of Chl *a* and Chl *b*.

Decay rate of luminescence for the four Chl species

Rise and decay curves of luminescence were measured on samples that exhibited different concentrations of Chl molecules (Fig. 3A); three different conditions were adopted. Photobleaching of samples was scarcely observed during measurements, which confirmed the reliability of our estimations. Observed decay curves were fitted using the following function:

$$I(t) = A \times (\exp(-k_1 t) - \exp(-k_2 t)),$$

where I(t) stands for singlet oxygen emission intensity at time t after the excitation pulse; k_1 is a decay time constant of singlet oxygen; k_2 is a decay time constant of Chl triplet state, and A is the amplitude of the exponential decay. Rise terms were almost identical in the four samples (200 to 210 ns, Table 1) and decay times were also very similar among the samples (49 to 55 μs, Table 1).

The time constants (k_1) observed were plotted as a function of Chl concentration, and quenching rate constants were calculated from plot slopes using a regression analysis (Fig. 3B). It is expected that the extrapolation of these regression lines to the zero Chl concentration would yield identical rates that would be dependent exclusively on the type of solvent. This was reproduced in our measurements, even if a difference of maximally ~10% was observed between Chl *a* and Chl *b* (data not shown). The resolved quenching rate constants were largest for Chl *a* (2.26×10^9 L mol^{-1} s^{-1}), whereas those of Chl *b*, Chl *d*, and

DV-Chl *a* were 0.54 $\times 10^9$, 1.33 $\times 10^9$, and 1.44 $\times 10^9$ L mol^{-1} s^{-1}, respectively (Table 1). This difference was dependent on the Chl species. The quenching rates of Chl *d* and DV-Chl *a* were comparable and were much larger than that of Chl *b*.

Discussion

Improvement of a detection system

The emission yield of singlet oxygen in solution is low [6] and the sensitivity of detection at 1275 nm using the systems available currently is not necessarily high. These facts led us to employ unusual measuring conditions, such as a high Chl concentration, high pulse intensity, and long exposure times. These induce aggregation of Chl molecules, saturation of absorption light upon excitation, and light-induced damage to samples. Furthermore, we were aware that an emission overlapped a weak luminescence from singlet oxygen (data not shown), even though the origin of emission was not identified. This emission hindered the accurate estimation of the yield of singlet oxygen. These factors led to difficulties in performing accurate measurements of singlet oxygen under the conditions used so far. In this study, we adopted a gated image intensifier as a detector, which presented the advantage of providing high sensitivity up to the near-infrared region and a gate function that eliminated the scattered light of the excitation pulse using a synchronous gate mode. It also enabled the selective detection of emissions from singlet oxygen. Furthermore, we adopted spectra-measuring conditions that included a low pulse intensity, a low Chl concentration, and a short exposure time (approximately 10 s). The combination of these factors allowed the improvement of our detection system and its adjustment to a condition that was appropriate for the measurement of singlet oxygen with a high S/N ratio (Fig. 2A and 2B).

Production and quenching of singlet oxygen in relation to the chemical structure of Chls

Differences in production and quenching may be closely related to the molecular structure of the Chl species. The side groups of Chl *a* include a vinyl group at the R3 position and a

methyl group at the R7 position; these groups are replaced with vinyl and formyl groups, respectively, in Chl *b*, and formyl and methyl groups, respectively, in Chl *d*. DV-Chl *a* contains an additional vinyl group at the R8 position, while its other side chains are identical to those of Chl *a* (see Scheme).

The yield of singlet oxygen production in Chl *d* in acetone was higher by approximately 20% than that of Chl *a* (Table 1). In contrast, the yield of Chl *b* was more than two folds of that of Chl *a*. A similar result was reported for Chl *a* and Chl *b* [13]. The effect of the additional vinyl group of DV-Chl *a* on singlet oxygen production was not significant; an yield of DV-Chl *a* was comparable to that of Chl *d*. These results showed clearly that the major factor that affects singlet oxygen production was the presence of a formyl group at the R7 position.

Chl *b* showed a very different property regarding quenching. The quenching rate of Chl *b* was one-fourth that of Chl *a* (Table 1). A lower quenching rate of Chl *b* compared with Chl *a* in a benzene solution was also reported [16]. Chl *d* and DV-Chl *a* showed a clear difference when compared with Chl *a* (Fig. 3B and Table 1), which suggests that side-group substitution at the R3 and R8 positions was effective. These results suggest clearly that the replacement of the group at the R7 position of Chl *a* with a formyl group induced a lower quenching rate.

The effect of side groups on the production and quenching processes of singlet oxygen have been reported [12, 13, 16], and a clear difference was shown between Chl *a* and Chl *b*. In this study, we added two chlorin-ringed Chl species, i.e., Chl *d* and DV-Chl *a*, to the comparison, and revealed for the first time the presence of a clear effect of the formyl group at position R7 of the chlorin-ringed Chl species. This site-specific effect of the formyl group suggested that one of properties of a side chain, i.e. the electron attracting property, is the main reason for the production and quenching processes of singlet oxygen through changes in the electronic states of molecules. In this study, we showed that Chl *a* produced a least amount of singlet oxygen and quenched it most effectively among the four Chl species; this property might be linked to its function, that is, Chl *a* is least suffered from photoinhibition

by singlet oxygen and thus is responsible for a key role in photoreactions in photosynthetic organisms. Theoretical considerations on this subject will be our next target.

Dynamics of Chls in relation to the quenching process

The quenching rates of singlet oxygen in Chl solutions were in the range of 10^9 L mol^{-1} s^{-1} (Table 1), which is comparable to diffusion-limited values and indicates a very fast decay. In addition, we did not observe bleaching of Chl solutions during measurements (data not shown). This suggests that singlet oxygen did not interact with Chl molecules, which may induce photobleaching of solutions. Based on these observations, we concluded that quenching occurred via a photophysical process rather than via a photochemical process. This is in accordance with a report on the rate constants of the reaction of singlet oxygen with Chl *a*; a sum of the reaction rate, which included physical and chemical reactions, was reportedly between 1.2×10^7 and 7.3×10^8 L mol^{-1} s^{-1}, whereas that of the chemical reaction alone was between 2.0×10^6 and 4.0×10^6 L mol^{-1} s^{-1} [16]. This indicates clearly that the physical process was much faster than the chemical process. However, the reason for the difference in the total reaction rate, i.e., less than one-third of our estimation, was not clear. The low rate of quenching by Chl *b* was attributed to photophysical properties.

The yield and quenching rate are closely related to the photophysical processes of individual Chl species. The yields of singlet oxygen in individual Chl samples relative to that of Chl *a* were very different: 2.24, 1.20, and 1.22 for Chl *b*, Chl *d*, and DV-Chl *a*, respectively. The rise times of singlet oxygen production were estimated as approximately 200 ns in all samples (Fig. 3A and Table 1), which suggests strongly that the energy-transfer time from a triplet state to molecular oxygen was almost the same, irrespective of Chl species. Decay times of singlet oxygen were also similar among the Chl species (approximately 50 μsec, Fig. 3A and Table 1). The consistency of the rise and decay times in all samples resulted in an absence of significant differences in the observed emission spectra. Therefore, we concluded that the differences in singlet oxygen yield among the four Chl species did not arise from

variation of energy transfer time or of quenching rates; rather, it seems to have stemmed from the yield of the triplet state, i.e., the yield of intersystem crossing. A previous report supports the presence of a difference in yield of intersystem crossing between Chl *a* and Chl *b* [12]. In addition, the fluorescence yield was lower for Chl *b* [17]. These differences in the photodynamic properties of these molecules may be the main reason for the differences observed for the singlet oxygen production yield.

We obtained clear results for the novel Chl species, Chl *d* and DV-Chl *a*, regarding the effect of the replacement of the side chain(s) of the chlorine-ringed Chls. A formyl group at the R7 position was most effective in the production and quenching of singlet oxygen. This was the first report that used four different Chl species; therefore, our estimation may represent a basis for comparison, as several studies on the yield and quenching of singlet oxygen by Chl species reported divergent findings [12, 13, 16].

Correlation with in vivo *phenomena*

Arabidopsis and *Synechocystis* species that contained DV-Chl *a* were highly sensitive to a high light intensity, and bleaching of Chl species was observed in the tissues or cells of these plants [8, 10]. If Chl *b* is involved in the photochemical reaction centers of PS II, it may produce a higher amount of singlet oxygen compared with Chl *a*, as suggested by the *in vitro* experiment. If this is the case, the use of Chl *b* as the primary electron donor may be very harmful for oxygenic photosynthetic organisms. There are no organisms that use Chl *b* as the primary electron donor, which may reflect the fact that Chl *b* produces large quantities of singlet oxygen. DV-Chl *a* may be used as an electron donor exclusively under low light conditions. A high-light-adapted *Prochlorococcus* sp. is present in the ocean [18]; this species evolved from a low-light-adapted species and, during the transition from a low-light-adapted organism to a high-light-adapted organism, an additional modification in the proteins of the reaction center may have been included to allow usage of DV-Chl *a* as an electron donor in PS II.

The *in vitro* experiments performed to assess the production and quenching of singlet oxygen did not allow us to conclude that the difference between MV-Chl *a* and DV-Chl *a* may induce a significant difference on the tolerance to high-light conditions. However, the *in vivo* phenomena are significantly different [8, 10]. This discrepancy should be resolved based on the measurements of singlet oxygen production on complexes isolated from cells or thylakoid membranes. This is a critical point and a target for future analyses.

Acknowledgments

The authors thank Prof. A. Tanaka and Dr. H. Ito, Hokkaido University for their kind gift of the mutant of *Synechocystis* sp. PCC 6803, and Dr. S. Akimoto, Kobe University, for his critical reading of the manuscript. This work was supported by a Grant-in-Aid for the Creative Research from the Japanese Society for Promotion of Science (JSPS) to MM (Grant No. 17GS0314), and in part by a Grant-in-Aid for Scientific Research from the Ministry of Education of Japan to TT (21570038).

References

[1] K. Asada, Annu. Rev. Plant Physiol. Plant Mol. Biol. 50 (1999) 601.

[2] B. Andersson, E.-M. Aro, Physiol. Plant. 100 (1997) 780.

[3] E.-M. Aro, I. Virgin, B. Andersson, Biochim. Biophys. Acta 1143 (1993) 113.

[4] A.H. Salter, I. Virgin, A. Hagman, B. Andersson, Biochemistry 31 (1992) 3990.

[5] R. Barbato, C.A. Shipton, G.M. Giacometti, J. Barber, FEBS Lett. 290 (1991) 162.

[6] O. Shimizu, J. Watanabe, K. Imakubo, S, Naito, Chem. Lett. 28 (1999) 67.

[7] S. Satoh, M. Ikeuchi, M. Mimuro, A. Tanaka, J. Biol. Chem., 276 (2001) 4293.

[8] H. Ito, M. Yokono, R. Tanaka, A. Tanaka, J. Biol. Chem. 283 (2008) 9002.

[9] T. Tomo, S. Akimoto, H. Ito, T, T. Tsuchiya, M. Fukuya, A. Tanaka, M. Mimuro, Biochim. Biophys. Acta 1787 (2009) 191.

[10] N. Nagata, R. Tanaka, S. Satoh, A. Tanaka, Plant Cell 17 (2005) 233.

[11] A.A. Krasnovsky, Jr., P. Cheng, R.E. Blankenship, T.A. Moore, D. Gust, Photochem. Photobiol.57 (1993) 324.

[12] C. Tanielian, C. Wolff, J. Phys. Chem. 99 (1995) 9825.

[13] H. Kuepper, R. Dedic, A. Svoboda, J. Hala, P.M.H. Keoneck, Biochim. Biophys. Acta 1572 (2002) 107.

[14] R.W. Redmond, J.N. Gamlin, Photochem. Photobiol. 70 (1999) 391.

[15] T. Tomo, T. Okubo, S. Akimoto, H. Miyashita, T. Tsuchiya, T. Noguchi, M. Mimuro, Proc. Natl. Acad. Sci. U. S. A. 104 (2007) 7283.

[16] F. Wilkinson, W.P. Helman, A.B. Ross, J. Phys. Chem. Ref. Data 24 (1995) 663.

[17] G. Weber, F.W.J. Teale, Trans. Faraday Soc. 53 (1957) 646.

[18] G. Rocap, F.W. Larimer, J. Lamerdin, S. Malfatti, P. Chain, N.A. Ahlgren, A. Arellano, M. Coleman, L. Hauser, W.R. Hess, Z.I. Johnson, M. Land, D. Lindell, A.F. Post, W. Regala, M. Shah, S.L. Shaw, C. Steglich, Ma.B. Sullivan, C.S. Ting, A. Tolonen, E.A. Webb, E. R. Zinser, S.W. Chisholm, Nature, 424 (2003) 1042.

Figure legends

Scheme. Molecular structure of the four Chl species.

Fig. 1. Experimental setups for the measurement of singlet oxygen. A) Spectrum measurement setup and B) decay curve measurement setup.

Fig. 2. Emission spectra of singlet oxygen in the four kinds of Chl species in acetone solution. A) Emission spectra of singlet oxygen in Chl *a* and B) emission spectra of singlet oxygen in the four Chl samples in acetone. Spectra were normalized to the intensity observed at 1,275 nm.

Fig. 3. (A) Rise and decay curves of singlet oxygen in Chl *a* in acetone solution and (B) estimation of the quenching rate constant in the four Chl species in acetone solution.

Table 1: Characterization of singlet oxygen produced in the four Chl species.

	$^1O_2$ yield (relative to Chl *a*)	Rise term (ns)	Decay term (μs)	Quenching rate (10^9 dm^3 mol^{-1} s^{-1})
Chl *a*	1.00	200	50	2.26
Chl *b*	2.24	200	55	0.54
Chl *d*	1.20	210	53	1.33
DV-Chl *a*	1.22	200	49	1.44

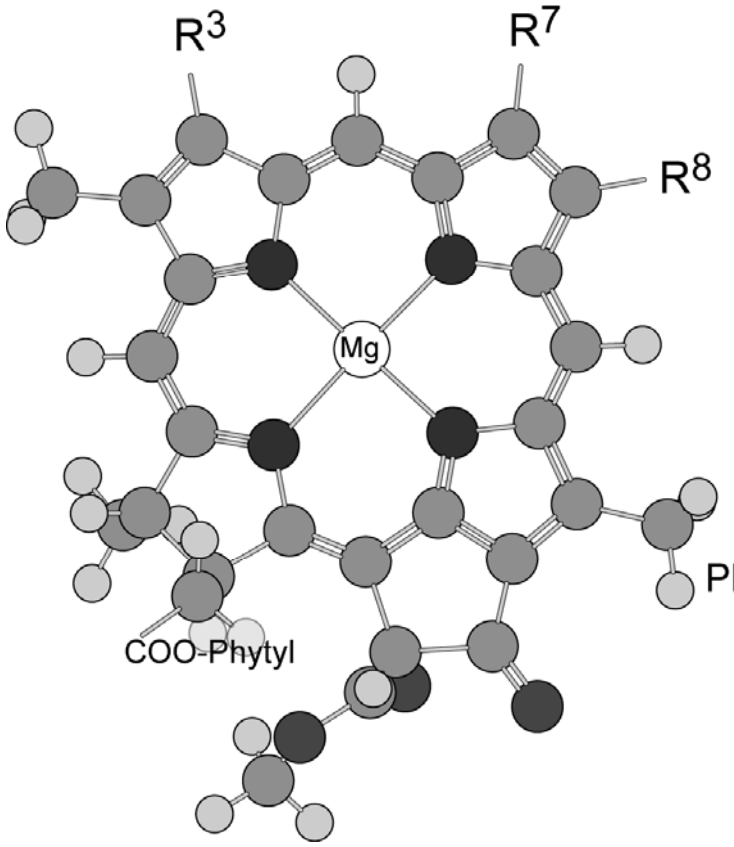

Chl *a*: R^3=CH=CH_2, R^7=CH_3, R^8=$CHCH_3$

DV-Chl *a*: R^3=CH=CH_2, R^7=CH_3, R^8=CH=CH_2

Chl *b*: R^3=CH=CH_2, R^7=CHO, R^8=$CHCH_3$

Chl *d*: R^3=CHO, R^7=CH_3, R^8=$CHCH_3$

Pheophytin *a*: R^3=CH=CH_2, R^7=CH_3, R^8=$CHCH_3$,
– Mg (replaced with two H)

Scheme.

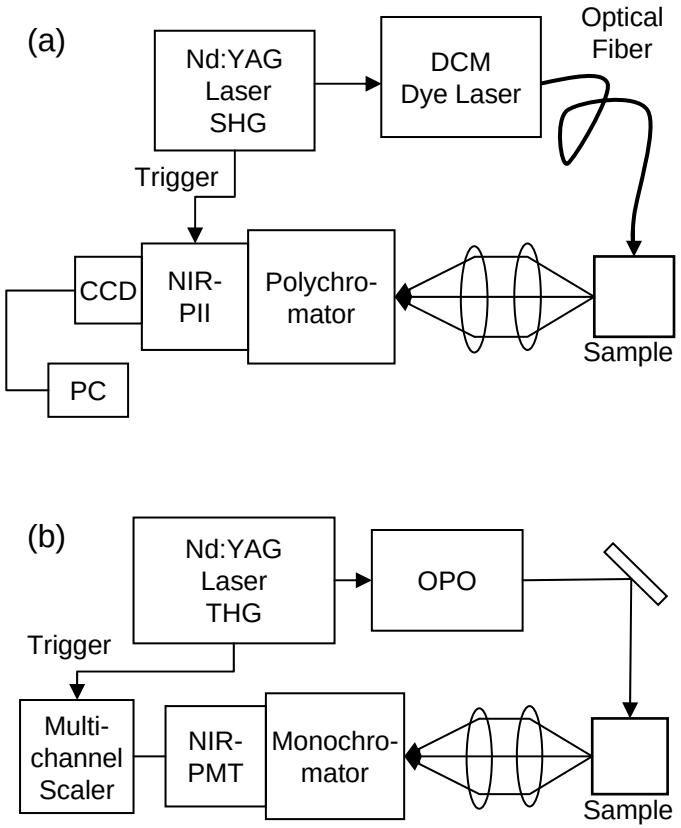
(a)
Nd:YAG
Laser
SHG
DCM
Dye Laser
Optical
Fiber
Trigger
CCD
NIR-
PII
Polychro-
mator
Sample
PC
(b)
Nd:YAG
Laser
THG
OPO
Trigger
Multi-
channel
Scaler
NIR-
PMT
Monochro-
mator
Sample

Fig. 1.

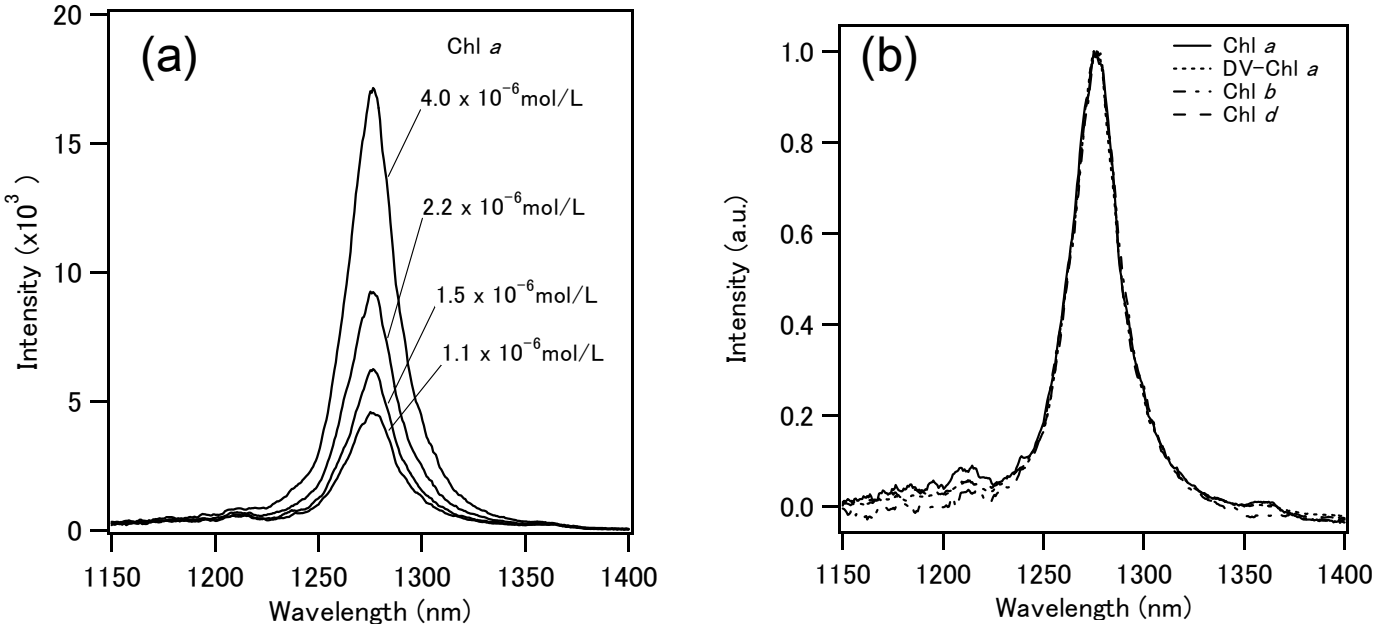
(a)
Chl a
4.0 x 10^-6mol/L
2.2 x 10^-6mol/L
1.5 x 10^-6mol/L
1.1 x 10^-6mol/L
Intensity (x10^3)
Wavelength (nm)
(b)
Chl a
DV-Chl a
Chl b
Chl d
Intensity (a.u.)
Wavelength (nm)

Fig. 2.

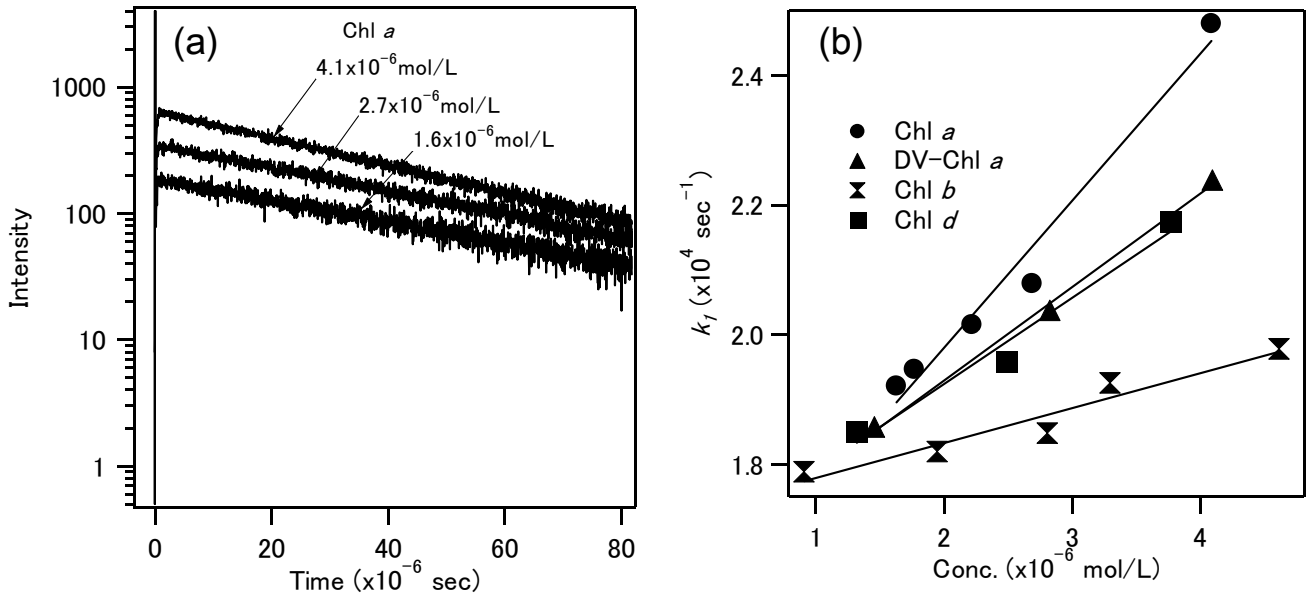
(a)
Chl a
4.1x10^-6mol/L
2.7x10^-6mol/L
1.6x10^-6mol/L
Intensity
1000
100
10
1
0
20
40
60
80
Time (x10^-6 sec)
(b)
Chl a
DV-Chl a
Chl b
Chl d
k1 (x10^4 sec^-1)
2.4
2.2
2.0
1.8
1
2
3
4
Conc. (x10^-6 mol/L)

Fig. 3.